Metastable He_2^- ions formed by two-electron attachment to the excited He_2^+ $^2\Sigma_g^+$ $(1\sigma_g^2 2\sigma_g^1)$ core

Ludwik Adamowicz

Department of Chemistry, University of Arizona, Tucson, Arizona 85721

Tadeusz Pluta

Department of Chemistry, Memphis State University, Memphis, Tennessee 38152

Four metastable states ($1\,^4\Pi_u$, $2\,^4\Pi_u$, $^4\Phi_u$, and ^4I_u), resulting from two-electron attachments to the excited He_2^+ core ($^2\Sigma_g^+$), are characterized using the numerical Hartree-Fock method. It is determined that such metastable states are formed when both valence electrons are placed into equally diffused orbitals, which have bonding charter, and whose angular momentum quantum numbers do not differ by more than 1.

I. INTRODUCTION

The determination of the interaction energy of two helium atoms has been a problem frequently attempted by quantum chemists. Although most of the attention has been paid to the van der Waals region [1], there have also been numerous studies of the repulsion portion of the interaction potential for both the ground and excited states [2–5]. Quantum calculations on the He_2 molecule are very demanding, especially for large internuclear separations, due to very small bonding effects. In particular, the basis-set superposition error (BSSE) presents a significant problem, and extended, well-optimized basis sets are usually necessary to obtain meaningful results.

Even more challenging than calculations for the neutral helium dimmer are calculations of a metastable He_2^- anion. Here, not only the core dissociation has to be described accurately but one also needs to properly represent the diffused character of the two valence electrons, which occupy Rydberg-like orbitals. The theoretical interest in relatively long-lived metastable states of He_2^- was prompted by the discovery of one of those states ($^4\Pi_g$) by Bea, Coggiola and Peterson [5], and its subsequent characterization by Kvale *et al.* [6]. The measurements were accomplished using a new experimental technique, called "excimer" autodetachment [7,8]. An advantage of this technique is the possibility of accurately measuring the energy of a transition from the vibrational levels of the bound metastable state of the He_2^- anion into the repulsive continuum of the He_2 ground state.

Theoretical works on the $^4\Pi_g$ $(1\sigma_g^2\,1\sigma_u^1\,2\sigma_g^1\,1\pi_u^1)$ metastable state of He_2^- were reported by Michels [9,10] who used the configuration interaction method, and by us [11,12] where the coupled cluster method and numerical orbital techniques were employed. These studies indicate that the principle of the formation of this state rests in a two-electron attachment to the He_2^+ core, which results in the formation of a quartet state, where both valence electrons occupy very diffused orbitals with bonding character. The similar degree of diffuseness of these or-

bitals is the key feature which facilitates the stability of the electronic structure of the metastable anion. If one of the orbitals were less diffused than the other, it would result in a reduction of the attractive nuclear potential felt by the more diffused electron and, in consequence, in its ejection from the stationary orbit. We have recently demonstrated [13] that this interesting phenomenon leads to the formation of two metastable Rydberg-like excitations of He_2^-, the $^4\Phi_g$ and ^4I_g states, corresponding to the following electronic configurations: $(1\sigma_g^2,1\sigma_u^1\,1\pi_u^1\,1\sigma_g^1)$ and $(1\sigma_g^2\,1\sigma_u^1\,1\delta_g^1,1\phi_u^1)$. The quantum-mechanical calculations on these states were among a number of similar calculations on possible configurations of He_2^- with the $(1\sigma_g^2\,1\sigma_u^1)$ core. Most of these calculations failed to produce spatially bound electronic states. As a result of this investigation, we formulated the following characterization of metastable states of He_2^-.

(i) The electronic structure of these states can be described as the He_2^+ core in its ground state with two valence electrons located on diffused orbits forming a quartet state.

(ii) Both valence electrons are bound if the valence shells they occupy have bonding character (i.e., no nodes in the perpendicular symmetry plane) and their angular quantum numbers do not differ by more than 1.

(iii) Both valence shells have a similar level of diffuseness. In effect, the attractive force of the core is similar for both valence electrons.

Following the above study, a question was raised whether a similar pattern of metastable anionic states will exist when the He_2^+ core is excited from the ground state, $^2\Sigma_u^+$ $(1\sigma_g^2 1\sigma_u^1)$, to the first excited state, $^2\Sigma_g^+$ $(1\sigma_g^2 2\sigma_g^1)$. One would expect that the promotion of the electron from the $1\sigma_u$ orbital to the $2\sigma_g$ orbital will result in a more diffused core and, in consequence, the metastable anionic states should be more spatially contracted than similar states formed with the He_2^+ core in its ground state. In this report we present quantum-mechanical calculations performed with the use of the numerical Hartree-Fock (NHF) method, which enabled

us to characterize several new metastable states of He$_2^-$ containing the excited He$_2^+$ core. As a result, we were able to evaluate the stability of these states with respect to the corresponding states of the neutral He$_2$ molecule.

The paper is organized as follows: Section II contains a brief description of the computational method used in this work, Sec. III presents numerical results for the metastable states of He$_2^-$ and "parent states" of the He$_2$ neutral. The work is summarized in Sec. IV.

II. DESCRIPTION OF THE METHOD

In the present study we used the diatomic numerical MCSCF program [14], which also enables us to perform single-configuration NHF calculations. The molecular orbitals in the numerical MCSCF method are represented as partial-wave expansions in elliptic coordinates with numerical radial components X:

$$\Psi^M(\zeta,\eta,\phi) = \sum_{L=M} X_L^M(\zeta) Y_L^M(\eta,\phi) , \qquad (1)$$

where

$$\zeta = (r_a + r_b)/R , \quad 1 \leq \zeta \leq \infty ,$$

$$\eta = (r_a - r_b)/R , \quad -1 \leq \eta \leq 1 ,$$

$$\phi , \quad 0 \leq \phi \leq 2\pi ,$$

and r_a and r_b are the scalar distances of the point in the space from the nucleic a and b, respectively, ϕ is the angle of rotation about the internuclear axis, and R is the internuclear separation.

In the conventional MCSCF approach, molecular orbitals are represented by truncated basis-set expansions. The error introduced by the truncation can be serious if an improper basis set is chosen. The numerical MCSCF method avoids this deficiency by solving the Fock equations for the radial components X on a densely spaced grid of points. The resulting molecular orbitals are essentially exact because the monotonic convergence of the partial-wave expansion (1) enables one to control the truncation error.

Use of the NHF method eliminates the basis-set superposition error and virtually alleviates the basis-set incompleteness problem. This is particularly important when the electronic structure under consideration possesses significantly diffused character. In addition, in the NHF method, the tendency for an electron to leave the system and escape to the continuum is clearly manifested by the increasing size of the corresponding orbital and its orbital energy rising and approaching zero. This feature was particularly instrumental in the present study, since the question raised with regard to each metastable state was whether it remains spatially bound or unbound.

III. RESULTS

As mentioned above, two electrons should remain bound to the He$_2^+$ core if they can be kept sufficiently diffused and none of them has a greater tendency to contract towards the nuclei. The search was conducted with the NHF method and our goal was to converge the pro-
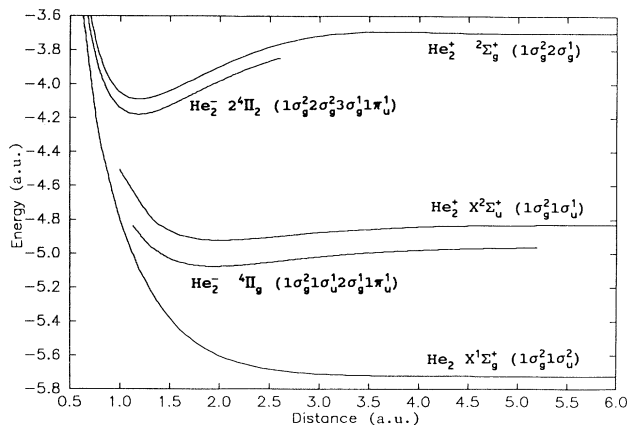
FIG. 1. NHF energy curves for the following states: He$_2$ $X\,^1\Sigma_g^+$ ($1\sigma_g^2 1\sigma_u^2$), He$_2^+$ $X\,^2\Sigma_u^+$ ($1\sigma_g^2 1\sigma_u^1$), He$_2^+$ $^2\Sigma_g^+$ ($1\sigma_g^2 2\sigma_g^1$), He$_2^-$ $^4\Pi_g$ ($1\sigma_g^2 1\sigma_u^1 2\sigma_g^1 1\pi_u^1$), and He$_2^- + 2\,^4\Pi_2$ ($1\sigma_g^2 2\sigma_g^2 3\sigma_g^1 1\pi_u^1$).

cedure to states which had the He$_2^+$ $^2\Sigma_g^+$ ($1\sigma_g^2 2\sigma_g^1$) excited core, and in which both valence electrons occupied spatially confined orbitals with negative orbital energies. Several possible configurations have been investigated for a wide range of internuclear separations. Similarly, as for the He$_2^+$ ground-state core [13], the states, in which the valence shells possessed angular momentum quantum numbers different by more than one (e.g., σ and δ) failed to converge to spatially bound states. This manifested itself in the calculations by a significant contraction of the orbital with smaller angular momentum and a simultaneous expansion of the other orbital. Also, we have not accomplished convergence for the states with one or both valence electrons occupying antibonding orbitals (π_g, δ_u, ϕ_u, etc.), except for the $1\,^4\Pi_u$ ($1\sigma_g^2 2\sigma_g^1 1\sigma_u^1 1\pi_g^1$) state at very short internuclear distances. Only when both elec-
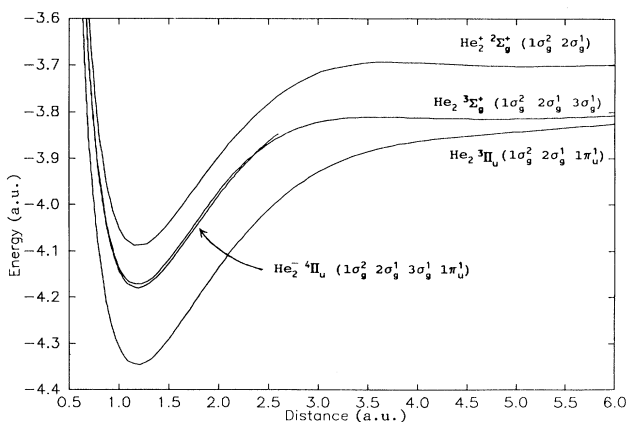
FIG. 2. Energy curves for the $2\,^4\Pi_u$ ($1\sigma_g^2 2\sigma_g^1 3\sigma_g^1 1\pi_u^1$) metastable state of He$_2^-$, corresponding "parent" states $^3\Sigma_g^+$ ($1\sigma_g^2 2\sigma_g^1 3\sigma_g^1$) and $^3\Pi_u$ ($1\sigma_g^2 2\sigma_g^1 1\pi_u^1$) of He$_2$, and the $^2\Sigma_g^+$ ($1\sigma_g^2 2\sigma_g^1$) state of He$_2^+$.

TABLE I. He_2^- $1\,^4\Pi_u$ $(1\sigma_g^2 2\sigma_g^1 1\sigma_u^1 1\pi_g^1)$. Total HF energy and orbital energies at selected internuclear separations. All entries in atomic units.

R	E_{HF}	$\varepsilon(1\sigma_g)$	$\varepsilon(2\sigma_g)$	$\varepsilon(1\sigma_u)$	$\varepsilon(1\pi_g)$
0.25	+3.515 818	−4.333 87	−0.527 77	−0.006 77	−0.002 36
0.3	−1.288 830	−4.164 81	−0.516 87	−0.006 88	−0.002 25
0.4	−1.233 287	−3.853 51	−0.495 49	−0.007 20	−0.001 89
0.45	−1.975 830	−3.712 35	−0.485 15	−0.007 46	−0.001 61
0.5	−2.520 264	−3.580 60	−0.475 12	−0.007 90	−0.001 19
0.51	−2.611 024	−3.555 36	−0.473 19	−0.008 04	−0.001 07
0.525	−2.737 650	−3.518 18	−0.470 36	−0.008 31	−0.000 85

trons occupied bonding orbitals (the orbitals with no nodes in the perpendicular symmetry plane of the molecule) and their angular quantum numbers were different by one did we obtain spatially confined states. In these cases, both valence orbitals possessed negative orbital energies. The He_2^- states, for which successful convergence was accomplished, are the following:

$$1\,^4\Pi_u \ (1\sigma_g^2 2\sigma_g^1 1\sigma_u^1 1\pi_g^1) \ ,$$

$$2\,^4\Pi_u \ (1\sigma_g^2 2\sigma_g^1 3\sigma_g^1 1\pi_u^1) \ ,$$

$$^4\Phi_u \ (1\sigma_g^2 2\sigma_g^1 1\pi_u^1 1\delta_g^1) \ ,$$

and

$$^4I_u (1\sigma_g^2 2\sigma_g^1 1\delta_g^1 1\phi_u^1) \ .$$

All of the above states except the first one are analogical to the previously studied metastable states of He_2^- containing the ground state He_2^+ Σ_u^+ $(1\sigma_g^2 1\sigma_u^1)$ core. The most significant difference is that, while the equilibrium internuclear distance for the former states were located near 2.0 a.u., for the present states the equilibrium separations are much shorter and are located around 1.2 a.u. One can assess this difference upon examining Fig. 1 where we present the comparison of the repulsive energy curve for the ground state of the neutral He_2 cluster, the energy curves of the ground state and the first excited state of He_2^+, the curve for the long-lived He_2^- $^4\Pi_g$ state studied earlier [5,9,10], and the curve of the He_2^- $^4\Pi_g$ state obtained in the present calculations. Below we discuss the characteristic features of the new metastable states.

A. $1\,^4\Pi_u$ $(1\sigma_g^2 2\sigma_g^1 1\sigma_u^1 1\pi_g^1)$

This metastable state is unique for the $(1\sigma_g^2 2\sigma_g^1)$ core and does not occur for the $(1\sigma_g^2 1\sigma_u^1)$ core. The values of the total energy of He_2^- in this state for selected internuclear separations are presented in Table I, along with the corresponding orbital energies. The expectation values of the squared distance between the electron and the center of the molecule ($\langle R^2 \rangle$) for all occupied orbitals are shown in Table II. Upon examining the tables, one notices that the anion remains bound only for very short internuclear separations. At about 0.525 a.u., the electron occupying the $1\pi_g$ orbital escapes from the system. This can be seen by examining the $1\pi_g$ orbital energy, which rapidly approaches zero, and the $\langle R^2 \rangle$ value, which increases significantly near 0.525 a.u. Interestingly, unlike the other metastable states of He_2^-, both valence shells for the $1\,^4\Pi_u$ state have antibonding character.

The relative stability of the $1\,^4\Pi_u$ state with respect to its "parent" states of the He_2 neutral molecule and the He_2^+ cation can be evaluated by comparing the total energies from Table I with the corresponding energies in Table III, where the NHF energies for He_2^+ and He_2 are shown. At the internuclear distance of 0.5 a.u., the anion is bound with respect to the $^2\Sigma_g$ He_2^+ state, but unbound with respect to both the $^3\Sigma_u^+$ $(1\sigma_g^2 2\sigma_g^1 1\sigma_u^1)$ and $^3\Pi_g$ $(1\sigma_g^2 2\sigma_g^1 1\pi_g^1)$ states of the He_2 neutral molecule.

B. $2\,^4\Pi_u$ $(1\sigma_g^2 2\sigma_g^1 3\sigma_g^1 1\pi_u^1)$

This metastable state has the same symmetry as the previously discussed state but slightly lower total energy

TABLE II. He_2^- $1\,^4\Pi_u$ $(1\sigma_g^2 2\sigma_g^1 1\sigma_u^1 1\pi_g^1)$. Expectation values of $\langle R^2 \rangle$ for the occupied orbitals at selected internuclear separations. All entries are in atomic units.

R	$\langle 1\sigma_g \rangle$	$\langle 2\sigma_g \rangle$	$\langle 1\sigma_u \rangle$	$\langle 1\pi_g \rangle$
0.25	0.300 09	6.906 9	764.48	930.01
0.3	0.320 95	7.140 0	754.81	933.74
0.4	0.366 33	7.628 9	728.73	954.12
0.45	0.390 54	7.881 5	710.69	979.62
0.5	0.415 68	8.138 6	686.06	1 037.6
0.51	0.420 81	8.190 6	679.33	1 060.3
0.525	0.428 58	8.269 0	667.10	1 111.4

TABLE III. Total NHF energy for He$_2^+$ and He$_2$ excited states (in atomic units).

R	He$_2^+$ [$1\sigma_g^2 2\sigma_g^1$]	He$_2$ [$1\sigma_g^2 2\sigma_g^1 \ldots$] [$\ldots 3\sigma_g^1$]	[$\ldots 1\sigma_u^1$]	[$\ldots 1\pi_g^1$]	[$\ldots 1\pi_u^1$]	[$\ldots 1\delta_g^1$]	[$\ldots 1\phi_u^1$]
0.5	−2.482 426	−2.574 513	−2.562 930	−2.540 177	−2.736 175	−2.539 925	−2.513 680
0.7	−3.601 951	−3.690 854	−3.694 936	−3.660 368	−3.859 294	−3.659 834	−3.633 198
0.9	−3.975 839	−4.061 943	−4.087 734	−4.035 049	−4.233 942	−4.034 103	−4.007 076
1.0	−4.049 002	−4.133 831	−4.170 248	−4.108 657	−4.306 668	−4.107 450	−4.080 232
1.1	−4.082 507	−4.166 138	−4.211 999	−4.142 543	−4.339 314	−4.141 135	−4.113 731
1.2	−4.090 718	−4.173 217	−4.227 206	−4.151 369	−4.346 321	−4.149 519	−4.121 933
1.3	−4.082 803	−4.164 235	−4.225 140	−4.144 006	−4.336 926	−4.141 771	−4.114 011
1.4	−4.064 765	−4.145 186	−4.211 965	−4.126 554	−4.317 190	−4.123 890	−4.095 963
1.6	−4.013 012	−3.091 568	−4.167 613	−4.076 080	−4.261 571	−4.072 424	−4.044 188
1.8	−3.954 316	−4.031 216	−4.113 999	−4.018 794	−4.198 623	−4.013 967	−3.985 465
2.0	−3.897 397	−3.973 007	−4.060 459	−3.963 390	−4.137 253	−3.957 226	−3.928 510
2.5	−3.783 181	−3.869 253	−3.949 063	−3.852 988	−4.011 408	−3.842 989	−3.814 142
3.0	−3.716 673	−3.822 683	−3.876 868	−3.788 169	−3.930 521	−3.774 857	−3.747 317
4.0	−3.694 891	−3.812 437	−3.821 006	−3.760 315	−3.863 329	−3.747 490	−3.725 034
6.0	−3.698 958	−3.807 494	−3.814 296	−3.767 177	−3.825 005	−3.747 672	−3.728 295
7.0	−3.689 182	−3.795 137	−3.806 839	−3.760 046	−3.805 863	−3.736 315	−3.718 046

TABLE IV. He$_2^-$ $2\,^4\Pi_u$ ($1\sigma_g^2 2\sigma_g^1 3\sigma_g^1 1\pi_u^1$). Total HF energy and occupied orbital energies at selected internuclear separations. All entries in atomic units.

R	E_{HF}	$\varepsilon\,(1\sigma_g)$	$\varepsilon\,(2\sigma_g)$	$\varepsilon\,(3\sigma_g)$	$\varepsilon\,(1\pi_u)$
0.5	−2.577 685	−3.462 49	−0.371 15	−0.027 18	−0.007 38
0.7	−3.695 468	−3.027 55	−0.341 80	−0.025 06	−0.008 73
0.9	−4.067 678	−2.698 30	−0.317 51	−0.023 38	−0.009 74
1.0	−4.140 028	−2.563 46	−0.306 93	−0.022 67	−0.010 15
1.1	−4.172 740	−2.444 49	−0.297 23	−0.022 03	−0.010 50
1.2	−4.180 176	−2.339 08	−0.288 31	−0.021 44	−0.010 80
1.3	−4.171 505	−2.245 30	−0.280 09	−0.020 91	−0.011 06
1.4	−4.152 730	−2.161 59	−0.272 50	−0.020 42	−0.011 29
1.6	−4.099 553	−2.019 26	−0.258 96	−0.019 56	−0.011 64
1.8	−4.039 497	−1.903 80	−0.247 32	−0.018 84	−0.011 90
2.0	−3.981 276	−1.809 17	−0.237 33	−0.018 23	−0.012 05
2.5	−3.864 247	−1.633 55	−0.218 13	−0.017 69	−0.011 16
2.6	−3.846 75	−1.598 70	−0.212 34	−0.019 28	−0.008 47

TABLE V. He$_2^-$ $2\,^4\Pi_u$ ($1\sigma_g^2 2\sigma_g^1 3\sigma_g^1 1\pi_u^1$). Expectation values of $\langle R^2 \rangle$ for occupied orbitals at selected internuclear separations. All entries in atomic units.

R	$\langle 1\sigma_g \rangle$	$\langle 2\sigma_g \rangle$	$\langle 3\sigma_g \rangle$	$\langle 1\pi_u \rangle$
0.5	0.415 99	8.100 8	123.47	193.42
0.7	0.524 91	9.117 0	131.99	185.98
0.9	0.646 32	10.147	140.12	182.98
1.0	0.711 67	10.664	144.06	182.50
1.1	0.780 22	11.181	147.92	182.48
1.2	0.852 05	11.698	151.72	182.84
1.3	0.927 31	12.214	155.44	183.50
1.4	1.006 1	12.729	159.10	184.42
1.6	1.175 2	13.751	166.23	186.85
1.8	1.360 5	14.755	173.14	189.91
2.0	1.563 7	15.723	179.82	193.53
2.5	2.159 9	17.675	190.55	209.94
2.6	2.297 4	17.880	177.94	233.35

TABLE VI. $He_2^- \; ^4\Phi_u$ ($1\sigma_g^2 2\sigma_g^1 1\pi_u^1 1\delta_g^1$). Total HF energy and occupied orbital energies for selected internuclear separations. All entries in atomic units.

R	E_{HP}	$\varepsilon(1\sigma_g)$	$\varepsilon(2\sigma_g)$	$\varepsilon(1\pi_u)$	$\varepsilon(1\delta_g)$
0.5	$-2.552\,466$	$-3.502\,83$	$-0.403\,02$	$-0.020\,58$	$-0.000\,98$
0.7	$-3.672\,087$	$-3.063\,33$	$-0.369\,78$	$-0.020\,41$	$-0.001\,04$
0.9	$-4.045\,919$	$-2.729\,88$	$-0.341\,80$	$-0.20\,03$	$-0.001\,21$
1.0	$-4.119\,008$	$-2.593\,09$	$-0.329\,48$	$-0.019\,78$	$-0.001\,32$
1.1	$-4.152\,416$	$-2.472\,27$	$-0.318\,14$	$-0.019\,51$	$-0.001\,44$
1.2	$-4.160\,506$	$-2.365\,12$	$-0.307\,66$	$-0.019\,22$	$-0.001\,57$
1.3	$-4.152\,453$	$-2.269\,70$	$-0.297\,97$	$-0.018\,92$	$-0.001\,71$
1.4	$-4.134\,261$	$-2.184\,43$	$-0.288\,99$	$-0.018\,61$	$-0.001\,86$
1.6	$-4.082\,156$	$-2.039\,24$	$-0.272\,92$	$-0.017\,99$	$-0.002\,17$
1.8	$-4.023\,061$	$-1.921\,26$	$-0.259\,06$	$-0.017\,37$	$-0.002\,48$
2.0	$-3.965\,693$	$-1.824\,41$	$-0.247\,11$	$-0.016\,77$	$-0.002\,78$
2.5	$-3.850\,052$	$-1.647\,01$	$-0.225\,08$	$-0.015\,36$	$-0.003\,47$
3.0	$-3.781\,123$	$-1.521\,16$	$-0.217\,21$	$-0.014\,17$	$-0.003\,95$
4.0	$-3.753\,558$	$-1.331\,21$	$-0.245\,49$	$-0.012\,48$	$-0.004\,48$
6.0	$-3.751\,949$	$-1.258\,56$	$-0.247\,97$	$-0.010\,40$	$-0.004\,96$
8.0	$-3.726\,134$	$-1.254\,81$	$-0.216\,85$	$-0.009\,30$	$-0.004\,98$

(at 0.5 a.u.). A characteristic feature of this state is that it remains bound at a much wider range of internuclear distances. At about 2.6 a.u., the $1\pi_u$ electron leaves the system. This can be seen upon examining the dependency of the $1\pi_u$ orbital energy and the corresponding $\langle R^2 \rangle$ value on the internuclear distance presented in Tables IV and V. It is interesting to note that the orbital energy of the $1\pi_u$ orbital reaches a minimum at about 2.0 a.u. and the $\langle R^2 \rangle$ expectation value has a minimum around 1.1. a.u.

The relative stability of the $^4\Pi_u$ state can be evaluated upon examining the NHF energies of this state and the energies of the corresponding "parent" states of He_2 and He_2^+ plotted in Fig. 2. One sees that the anion is bound with respect to both He_2^+ ($^2\Sigma_g^+$) and He_2 ($^3\Sigma_g^+$) but un-

bound with respect to He_2 ($^3\Pi_u$). At about 2.4 a.u., the He_2^- curve crosses the He_2 ($2\sigma_g$) curve and above this point the anion becomes unstable. A characteristic feature of the He_2^+ and He_2 ($^3\Sigma_g^+$) curves is a hump with its peak around 3.5 a.u. A similar extremum has been observed before and was the subject of considerable interest among both experimentalists and theoreticians [15-19].

C. $^4\Phi_u$ ($1\sigma_g^2 2\sigma_g^1 1\pi_u^1 1\delta_g^1$) and ^4I_u ($1\sigma_g^2 2\sigma_g^1 1\delta_g^1 1\phi_u^1$)

The total energies, orbital energies, and the averaged values of $\langle R^2 \rangle$ for all occupied orbitals are presented in Tables VI-IX. These two states are very similar to the $^4\Phi_g$ ($1\sigma_g^2 1\sigma_u^1 1\pi_u^1 1\delta_g^1$) and ^4I_g ($1\sigma_g^2 1\sigma_u^1 1\delta_g^1 1\phi_u^1$), which we described previously [13]. Both valence electrons remain

TABLE VII. $He_2^- \; ^4\Phi_u$ ($1\sigma_g^2 2\sigma_g^1 1\pi_u^1 1\delta_g^1$). Expectation values of $\langle R^2 \rangle$ for occupied orbitals for selected internuclear separations (in atomic units).

R	$\langle 1\sigma_g \rangle$	$\langle 2\sigma_g \rangle$	$\langle 1\pi_u \rangle$	$\langle 1\delta_g \rangle$
0.5	0.415\,82	8.169\,3	177.90	361.14
0.7	0.524\,69	9.211\,9	177.86	354.99
0.9	0.646\,05	10.273	179.34	344.58
1.0	0.711\,38	10.807	180.50	338.73
1.1	0.779\,91	11.342	181.89	332.87
1.2	0.851\,72	11.877	183.47	327.23
1.3	0.926\,96	12.413	185.21	321.90
1.4	1.005\,8	12.949	187.08	316.95
1.6	1.174\,8	14.014	191.18	308.27
1.8	1.360\,2	15.063	195.67	301.24
2.0	1.563\,3	16.081	200.54	295.79
2.5	2.158\,5	18.233	214.81	289.28
3.0	2.896\,1	18.321	235.56	298.92
4.0	4.811\,8	11.307	293.01	352.08
6.0	9.958\,7	11.104	372.23	417.49
8.0	16.989	14.692	435.96	475.10

TABLE VIII. He$_2^-$ ^4I_u ($1\sigma_g^2 2\sigma_g^1 1\delta_g^1 1\phi_u^1$). Total HF energy and occupied orbital energies for selected internuclear separations. All entries are in atomic units.

R	E_{HF}	ε $(1\sigma_g)$	$\varepsilon + (2\sigma_g)$	$\varepsilon + (1\delta_g)$	ε $(1\phi_u)$
0.7	$-3.634\,314$	$-3.156\,00$	$-0.455\,03$	$-0.006\,79$	$-0.001\,66$
0.9	$-4.008\,315$	$-2.821\,95$	$-0.426\,74$	$-0.006\,85$	$-0.001\,63$
1.0	$-4.081\,530$	$-2.684\,75$	$-0.414\,20$	$-0.006\,87$	$-0.001\,62$
1.1	$-4.115\,085$	$-2.563\,52$	$-0.402\,56$	$-0.006\,90$	$-0.001\,61$
1.2	$-4.123\,341$	$-2.455\,90$	$-0.391\,77$	$-0.006\,93$	$-0.001\,59$
1.3	$-4.115\,470$	$-2.359\,98$	$-0.381\,72$	$-0.006\,95$	$-0.001\,59$
1.4	$-4.097\,471$	$-2.274\,20$	$-0.372\,36$	$-0.006\,97$	$-0.001\,58$
1.6	$-4.045\,784$	$-2.127\,88$	$-0.355\,42$	$-0.007\,01$	$-0.001\,56$
1.8	$-3.987\,137$	$-2.008\,7$	$-0.340\,58$	$-0.007\,04$	$-0.001\,55$
2.0	$-3.930\,245$	$-1.910\,52$	$-0.327\,51$	$-0.007\,06$	$-0.001\,54$
2.5	$-3.815\,955$	$-1.729\,09$	$-0.302\,45$	$-0.007\,05$	$-0.001\,54$
3.0	$-3.748\,922$	$-1.596\,09$	$-0.289\,99$	$-0.006\,88$	$-0.001\,58$
4.0	$-3.725\,438$	$-1.394\,19$	$-0.307\,88$	$-0.006\,22$	$-0.001\,81$
6.0	$-3.728\,092$	$-1.311\,77$	$-0.300\,48$	$-0.005\,79$	$-0.001\,90$
8.0	$-3.704\,837$	$-1.301\,79$	$-0.262\,69$	$-0.005\,51$	$-0.001\,90$

bound for all internuclear distances examined (0.5–8.0 a.u.). The valence shells have a significantly diffused character, more so for the ^4I_u state than for the $^4\Phi_u$ state. Both states are bound with respect to the He$_2^+$ ($^2\Sigma_g^+$). The $^4\Phi_u$ state is also bound with respect to the "parent" $^3\Delta_g$ state of He$_2$, but unbound with respect to the He$_2$ $^3\Pi_u$ state for all internuclear distances considered. The ^4I_u state follows the same pattern for the majority of the internuclear separations as the $^4\Phi_u$ state, i.e., remains bound with respect to the $^3\Phi_u$ state of He$_2$ but unbound with respect to the He$_2$ $^3\Delta_g$ state. However, beyond about 6.0 a.u. the $^4I_4$ state becomes unbound with respect to both the parent states of the neutral molecule.

D. Vibrational analysis

In Table X we present the spectroscopic constants evaluated based on the NHF energy curves obtained for

all the states of He$_2^+$, He$_2$, and He$_2^-$ considered in the present work. The results may help in an experimental attempt to measure the metastable states of He$_2^-$ formed with the excited He$_2^+$ core. An interesting, however rather understandable, observation which one can make upon examining the results is that the vibrations of the metastable He$_2^-$ are very similar to the vibrations of He$_2^+$. For example, the two-electron attachment alters the value of ω_e for He$_2^+$ by 46 cm^{-1} when the $^4\Pi_u$ state is formed, by 10 cm^{-1} when the $^4\Phi_u$ state is formed, and only by 7 cm^{-1} in the case of the ^4I_u state.

IV. CONCLUSIONS

The aim of the present work is to characterize the electronic structure of the He$_2^-$ metastable anions formed by two-electron attachments to the excited He$_2^+$ core with

TABLE IX. He$_2^-$ ^4I_u ($1\sigma_g^2 2\sigma_g^1 1\delta_g^1 1\phi_u^1$). Expectation values of $\langle R^2 \rangle$ for occupied orbitals for selected internuclear separations. All entries are in atomic units.

R	$\langle 1\sigma_g \rangle$	$\langle 2\sigma_g \rangle$	$\langle 1\delta_g \rangle$	$\langle 1\phi_u \rangle$
0.7	0.524\,27	9.113\,3	840.55	1\,116.7
0.9	0.645\,43	10.133	832.08	1\,110.3
1.0	0.710\,66	10.643	828.11	1\,107.5
1.1	0.779\,06	11.153	824.46	1\,104.5
1.2	0.850\,75	11.662	821.05	1\,101.8
1.3	0.925\,86	12.170	817.91	1\,099.2
1.4	1.004\,5	12.676	815.03	1\,097.0
1.6	1.173\,3	13.680	810.19	1\,092.7
1.8	1.358\,4	14.666	806.55	1\,089.5
2.0	1.561\,3	15.620	804.25	1\,087.4
2.5	2.156\,1	17.624	806.84	1\,091.1
3.0	2.894\,5	17.661	836.87	1\,124.2
4.0	4.809\,4	11.069	960.33	1\,248.5
6.0	9.955\,4	10.847	1\,071.9	1\,373.0
8.0	16.986	14.332	1\,171.2	1\,497.7

TABLE X. Vibrational analysis of He_2^+, He_2, and He_2^-.

| | R_e (a.u.) | E_e (a.u.) | ω_e (cm⁻¹) | $\omega_e X_e$ (cm⁻¹) | B_e (cm⁻¹) | α_e (cm⁻¹) | ΔG $(v+\frac{1}{2})$ (cm⁻¹) | | |
							$v=0$	$v=1$	$v=2$
				He_2^+					
$(1\sigma_g^2 2\sigma_g^1)$	1.190	−4.090753	4647	56.87	21.12	0.4629	4533	4421	4311
				He_2					
$(1\sigma_g^2 2\sigma_g^1 3\sigma_g^1)$	1.185	−4.173367	4708	56.71	21.36	0.4623	4596	4484	4373
$(1\sigma_g^2 2\sigma_g^1 1\sigma_u^1)$	1.195	−4.225196	5883	39.63	21.29	0.7520	5218	4647	4425
$(1\sigma_g^2 2\sigma_g^1 1\pi_g^1)$	1.195	−4.151378	4607	57.63	21.01	0.4680	4493	4379	4267
$(1\sigma_g^2 2\sigma_g^1 1\pi_u^1)$	1.185	−4.364651	4771	56.83	21.40	0.4427	4460	4552	4453
$(1\sigma_g^2 2\sigma_g^1 1\delta_g^1)$	1.195	−4.149546	4638	56.90	21.09	0.4629	4524	4412	4301
$(1\sigma_g^2 2\sigma_g^1 1\phi_u^1)$	1.195	−4.121969	4647	56.83	21.12	0.4628	4534	4422	4311
				He_2^-					
$(1\sigma_g^2 2\sigma_g^1 3\sigma_g^1 1\pi_u^1)$	1.190	−4.180284	4693	56.65	21.30	0.4614	4581	4469	4359
$(1\sigma_g^2 2\sigma_g^1 1\pi_u^1 1\delta_g^1)$	1.190	−4.160550	4657	56.72	21.16	0.4615	4545	4433	4327
$(1\sigma_g^2 2\sigma_g^1 1\delta_g^1 1\phi_u^1)$	1.195	−4.123375	4654	56.75	21.16	0.4622	4541	4429	4319

the use of the numerical Hartree-Fock method. This method offers a single-configuration basis-set error-free approximate solution of the electronic Schrödinger equation. The characteristic features of the metastable states examined in the present study are similar to the metastable states which are formed by two-electron attachments to the He_2^+ core in its ground state, which were examined in our previous studies [11,13]. However, we were not able to obtain a state which would remain bound with respect to both respective "parent" states of the neutral He_2 molecule, as was achieved for the $^4\Pi_g$ $(1\sigma_g^2 1\sigma_u^1 2\sigma_g^1 1\pi_u^1)$ metastable state. The present calculations show that, in order for the new metastable states to remain bound, the following have to apply.

(i) Both valence shells have to possess bonding character (i.e., no nodes in the perpendicular symmetry plane) and their angular quantum number should not differ by more than one.

(ii) Both valence shells have to possess a similar level of diffuseness.

An interesting question which one may ask pertains to the predicted lifetime of the He_2^- states characterized in this work. Decay-rate measurements by Bae, Coggiola, and Peterson [5] indicate that the He_2^- beam contained several states with different lifetimes ranging from less than 10^{-5} s to more than 10^{-4} s similar to those of the $J=\frac{1}{2}$, $\frac{3}{2}$, and $\frac{5}{2}$ fine-structure states of He^- ^4P. It is reasonable to assume that, because of the similarity of the

states calculated here to the He_2^- states with the ground state He_2^+ core described before, the lifetime of these new states will be similar provided that the He_2^+ core excitation is sufficiently long lived. The autodetachment spectrum in a system with an unbound final state such as He_2^- represents the decay rate as a function of the internuclear separation averaged over the observation time. Each of the presently characterized states has three fine-structure states with different J values, which have different intrinsic decay rates. Two states with the lowest J values are expected to decay primarily through spin-orbit coupling to negative-ion resonances in the doublet-spin manifold with typical intrinsic lifetimes of about 10 μs, which the highest-J state decays only through the weaker spin-spin interaction in the order of 100 μs [2,8].

Finally, there is an indication that the excited metastable states of He_2^- considered in this study may not only be a theoretical curiosity. It was recently discovered [20] that the He^- $(1s2p^3)$ shape resonance has an enormous effect on the photodetachment of metastable He^-. The He_2^- metastable states considered here may play a similar role in the photodetachment of metastable He_2^-.

ACKNOWLEDGMENTS

[1] J. H. Van Lenthe, J. G. C. M. Van Duijneveldt-van de Rijdt, and F. B. Van Duijneveldt, Adv. Chem. Phys. 57, 521 (1987); G. Chalasinski and M. Gutowski, Chem. Rev. 88, 943 (1988); B. Liu and A. D. McLean, J. Chem. Phys. 72, 3418 (1980); P. G. Burton, ibid. 70, 3112 (1979); M. Gutowski, J. Verbeek, J. H. Van Lenthe, and G. Chalasinski, Chem. Phys. 111, 271 (1987).

[2] G. H. Matsumoto, C. F. Bender, and E. R. Davidson, J.

Chem. Phys. 46, 402 (1967); P. E. Philipson, Phys. Rev. 125, 1980 (1962); J. H. Van Lenthe, R. J. Vos, J.G.C.M. Van Duijneveldt-Van de Rijdt, and F. B. Van Duijneveldt, Chem. Phys. Lett. 143, 435 (1988); D. J. Klein, J. Chem. Phys. 50, 5151 (1969); B. J. Garrison, W. H. Miller, and H. F. Schaefer, ibid. 59, 3193 (1973).

[3] K. K. Sunil, J. Lin, P. E. Siska, K. D. Jordan, and R. Shepard, J. Chem. Phys. 78, 6190 (1983).

[4] D. Konowalow and Byron H. Lengsfield III, J. Chem. Phys. **87**, 4000 (1987).

[5] Y. K. Bae, M. J. Coggiola, and J. R. Peterson, Phys. Rev. Lett. **52**, 747 (1984).

[6] T. J. Kvale, R. N. Compton, G. D. Alton, J. S. Thompson, and D. J. Pegg, Phys. Rev. Lett. **56**, 582 (1986).

[7] P. S. Drzaic, J. Marks, and J. I. Brauman, in *Gas Phase Ion Chemistry,* edited by M. T. Bowers (Academic, New York, 1984).

[8] Y. K. Bea, J. R. Peterson, H. H. Michels, and R. H. Hobbs, Phys. Rev. A **37**, 2778 (1988).

[9] H. H. Michels, Phys. Rev. Lett. **52**, 1413 (1984).

[10] H. H. Michels, Chem. Phys. Lett. **126**, 537 (1986).

[11] T. Pluta, R. J. Bartlett, and L. Adamowicz, Int. J. Quantum. Chem. Symp. **22**, 225 (1988).

[12] T. Pluta, R. J. Bartlett, and L. Adamowicz, Phys. Rev. A **40**, 2253 (1969).

[13] L. Adamowicz and T. Pluta, Chem. Phys. Lett. **179**, 517 (1991).

[14] E. A. McCullough, Jr., Chem. Phys. Lett. **24**, 55 (1974); J. Chem. Phys. **62**, 3991 (1975); L. Adamowicz and E. A. McCullough, Jr., *ibid.* **75**, 2475 (1981); E. A. McCullough, Jr., Comput. Phys. Rep. **4**, 267 (1986).

[15] R. S. Mulliken, Phys. Rev. **136A**, 962 (1964).

[16] S. L. Guberman and W. A. Goddard III, Chem. Phys. Lett. **14**, 460 (1972).

[17] S. L. Guberman and W. A. Goddard III, Phys. Rev. A **12**, 1203 (1975).

[18] R. M. Jordan, H. R. Siddiqui, and P. E. Siska, J. Chem. Phys. **84**, 6719 (1986).

[19] B. Brutschy and H. Haberland, Phys. Rev. **19**, 2232 (1979).

[20] H. P. Saha and R. N. Compton, Phys. Rev. Lett. **64**, 1510 (1990).